THE JOURNAL OF PHYSICAL CHEMISTRY B

ARTICLE

pubs.acs.org/JPCB

Hierarchical Nanostructures Self-Assembled from Diblock Copolymer/Homopolymer Blends with Supramolecular Interactions

Ying Zhuang, Liquan Wang, and Jiaping Lin*

Shanghai Key Laboratory of Advanced Polymeric Materials, Key Laboratory for Ultrafine Materials of Ministry of Education, State Key Laboratory of Bioreactor Engineering, School of Materials Science and Engineering, East China University of Science and Technology, Shanghai 200237, China

ABSTRACT: Self-assembly of **AB** diblock copolymer/**C** homopolymer blends with reversible supramolecular interactions was studied by real-space self-consistent field theory. The reversible bond is formed between the **B** free end of the **AB** diblock copolymers and one end of the **C** homopolymers, and thereby the supramolecular blends consist of the **AB** diblock copolymers, **C** homopolymers, and supramolecular **ABC** terpolymers. The constitutions of the blends are dependent on the bonding strength and blend ratio. The change of the bonding strength and blend ratio leads to a series of hierarchically ordered alternating nanostructures. In these alternating nanostructures, the **C** homopolymers exhibit a swollen effect on the **C** substructures, and the coordination number of **C** cylinders decreases as the bonding strength increases. To gain the information about the hierarchical nanostructures in details, one-dimensional density profiles were plotted. The results were finally compared with the existing experimental findings, and an agreement was shown. The obtained results provided an insight into the role of the supramolecular interactions on the hierarchical nanostructure formations.

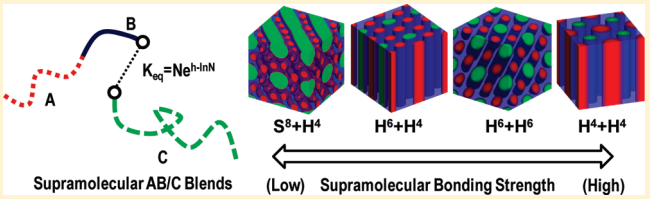

INTRODUCTION

Manufacture of advanced apparatus such as microelectronic components and solar cells requires the materials possessing hierarchical nanophase-separated structures.[1−5] For preparing hierarchical nanostructures, the self-assembly approach has progressed from **AB** diblock copolymer to more sophisticated **ABC** terpolymer systems.[6−10] However, the difficulty in synthesizing **ABC** terpolymers prevents the further applications in functional materials. Simply blending different polymers can overcome the difficulty of polymeric synthesis, but encounter another problem of macrophase separation.[11−17] Introduction of supramolecular interactions, such as hydrogen-bonds and ligands, into the blend system would effectively suppress the macrophase separation and encourage the self-assembly of molecules into hierarchical nanostructures.[18−23]

Up to now, most of the studies on polymer blends with supramolecular interactions involve the investigation of polymer miscibility.[24−29] For example, Matsushita et al. found an enhancement in the miscibility of the blends containing poly(styrene-*b*-2-vinylpyridine) (SP) and poly(4-hydroxystryene) (H) with supramolecular interactions, as compared to the poly(styrene-*b*-2-vinylpyridine) (SP)/poly(2-vinylpyridine) (P) blend system without supramolecular interactions.[24] The research area of supramolecular blends was further enriched in the several recent works.[20−23] Fredrickson et al. designed a supramolecular blend system based on poly(ethylene oxide)-*b*-poly(styrene-*r*-4-hydroxystyrene) and poly(styrene-*r*-4-vinylpyridine)-*b*-poly(methyl methacrylate).[23] This blend of copolymers was found to generate the square arranged nanostructures, which can enable the applications in integrated circuit manufacturing and nanotechnology. Their study reveals that the self-assembly of supramolecular blend system is an excellent strategy for the generation of novel hierarchical structures. In addition to this study, some other hierarchical nanostructures self-assembled from block copolymer/block copolymer blends based on supramolecular interactions were also reported.[20,21] However, the related studies concerning the formation of hierarchical nanostructures from the blend systems with supramolecular interactions are still limited, and many mechanisms behind the hierarchical nanostructure formation remain unclear. To provide a good understanding of the role of the supramolecular blends in generating hierarchical nanostructures and also offer a foundation for manufacturing advanced apparatus, we carried out a systematical study on the hierarchical structures self-assembled from a supramolecular blend by theoretical methods.

Because of the large parameter space that characterizes the supramolecular blend systems, the experimental exploration could be a very costly and time-consuming task. From this perspective, theories and simulations provide an important tool for the studies of the nanostructures formed by the blend system with supramolecular interactions. For example, random-phase approximation and Monte Carlo simulations have been employed to study diblock copolymer and graft copolymer based on supramolecular interactions.[30−35] In addition to these methods,

Received: March 8, 2011
Revised: May 3, 2011
Published: May 18, 2011

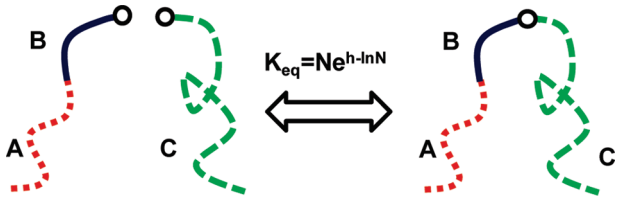

Figure 1. Schematic representation of **AB** diblock copolymer/**C** homopolymer blends in which terminal heterocomplementary bonding groups on the **B** and **C** blocks can reversibly bind to form a supramolecular **ABC** terpolymer.

self-consistent field theory (SCFT) is another powerful tool to study the equilibrium nanostructures.[36−46] Fredrickson et al. have extended the grand-canonical SCFT to investigate the phase behavior of supramolecular **AB** diblock copolymer and **ABA** triblock copolymer melts.[47,48] In their study, the volume fractions of the copolymers in the supramolecular systems were formulated with the supramolecular bonding strength. It was found that the phase behavior of the polymer melts is dependent on the bonding strength. Despite of these studies, scarcely theoretical investigation was concerned about the complex hierarchical nanostructures self-assembled from a supramolecular interaction based system.

In this work, we used the canonical SCFT to study the hierarchical nanostructures self-assembled from the blend system based on supramolecular interactions. The supramolecular blend system studied is a diblock copolymer (**AB**)/homopolymer (**C**) blend with supramolecular interaction. The **B** free end of **AB** diblock copolymers was considered to be reversibly connected to one end of **C** homopolymers, and thereby forms a supramolecular bond, as schematically shown in Figure 1. The supramolecular **AB**/**C** blend has been studied in experiments, which are important in practical applications.[24−28] However, the theoretical understanding of the underlying principle governing the formation of hierarchical structures needs to be further explored. The striking feature of the supramolecular bonds is tunable and reversible.[49−52] The supramolecular **AB**/**C** blend system performs as a simple blend system at weaker interactions, while the supramolecular systems behave like an **ABC** terpolymer system at stronger interactions. When the interactions are intermediate, the supramolecular systems appear to be more complex, which is a combination of **AB** diblock copolymer, **C** homopolymer, and **ABC** terpolymers. Therefore, the supramolecular bonding strength should have a marked effect on the morphology of the supramolecular blends. In addition, the blend ratio is another factor influencing the self-assembled nanostructures. In the work, both the effects of the bonding strength and blend ratio on the nanostructures were examined by using the SCFT method.

THEORETICAL METHOD

We consider an incompressible blend with volume V of **AB** diblock copolymers and **C** homopolymers. The heterocomplementary bonding groups at the free end of **B** block in **AB** diblock copolymer and one end of **C** homopolymer allow two different polymers to form a supramolecular **ABC** terpolymer with length $N = N_A + N_B + N_C$, where N_A, N_B, and N_C are the degrees of polymerization of **A** block, **B** block, and **C** homopolymer, respectively. Thus, in a supramolecular **ABC** terpolymer, the volume fraction of **A**, **B**, **C**, and **AB** blocks is $f_A = N_A/N$, $f_B = N_B/N$, $f_C = N_C/N$, and $f_{AB} = f_A + f_B$, respectively. Thus, $f_{ABC} = f_A + f_B + f_C = 1$. The generalization of our formalism to self-complementary bonding groups is straightforward. Each polymer segment in the incompressibility blend occupies a fixed volume ρ_0^{-1}. The chemical equilibrium of the bonding reaction is expressed by[47,48]

$$\frac{\nu_{ABC}}{\frac{\nu_{AB}}{f_{AB}}\frac{\nu_{Ch}}{f_C}} = K_{eq}/N = e^{h - \ln N} \tag{1}$$

where the free energy decrease for bonding in units of the thermal energy, k_BT, is denoted by h, and $K_{eq} = \exp(h)$ is an equilibrium constant. ν_{AB}, ν_{Ch}, and ν_{ABC} respectively represent the average volume fraction of the unbonded **AB** diblock copolymer, unbonded **C** homopolymer, and supramolecular **ABC** terpolymer at equilibrium state. The bonding constraints of eq 1 as well as incompressibility determine the average volume fractions, which are

$$\nu_{AB} = \frac{f_{AB}\cdot f_C\cdot(1-\nu_{Ch})}{f_{AB}\cdot f_C + \exp(h-\ln N)\cdot\nu_{Ch}} \tag{2}$$

$$\nu_{ABC} = \exp(h-\ln N)\cdot\frac{\nu_{AB}}{f_{AB}}\cdot\frac{\nu_{Ch}}{f_C} \tag{3}$$

The total volume fraction of **C** components in the system $\nu_{C,tot}$ is given by $\nu_{C,tot} = \nu_{Ch} + f_C\cdot\nu_{ABC}$

Within the SCFT model, the configuration of a single polymer is determined by a set of effective chemical potential fields w_i (i = **A**, **B**, and **C**). The potential fields w_i are conjugated to the density fields $\phi_i(\mathbf{r})$. The free energy density (in units of k_BT) for the polymer blend systems is

$$\begin{aligned} F = & -\frac{\nu_{AB}}{f_{AB}}\ln\frac{f_{AB}Q_{AB}}{\nu_{AB}V} - \frac{\nu_{Ch}}{f_C}\ln\frac{f_CQ_{Ch}}{\nu_{Ch}V} - \nu_{ABC}\ln\frac{Q_{ABC}}{\nu_{ABC}V} \\ & + \frac{1}{V}\int d\mathbf{r}\,[\chi_{AB}N\phi_A(\mathbf{r})\phi_B(\mathbf{r}) + \chi_{AC}N\phi_A(\mathbf{r})\phi_C(\mathbf{r}) \\ & + \chi_{BC}N\phi_B(\mathbf{r})\phi_C(\mathbf{r}) - w_A(\mathbf{r})\phi_A(\mathbf{r}) - w_B(\mathbf{r})\phi_B(\mathbf{r}) \\ & - w_C(\mathbf{r})\phi_C(\mathbf{r}) - \xi(\mathbf{r})(1-\phi_A(\mathbf{r}) - \phi_B(\mathbf{r}) - \phi_C(\mathbf{r}))] \end{aligned} \tag{4}$$

Here, $\xi(\mathbf{r})$ is the potential field that is invoked by incompressibility condition. χ_{ij} characterizes the interactions between i and j species. The single chain partition functions for the **AB** diblock copolymer, **C** homopolymer, and supramolecular **ABC** terpolymer are denoted by Q_{AB}, Q_{Ch}, and Q_{ABC}, respectively. The partition functions, Q_i, can be expressed in terms of propagators, $q_i(\mathbf{r},s)$, which are the single chain statistical weights for a continuous Gaussian chain of contour length s at position $\mathbf{r}$ and experiencing the w_i potential field. All single chain partition functions are written as $Q_i = \int d\mathbf{r}\, q_i(\mathbf{r},s)q_i^+(\mathbf{r},s)$ (i = **AB**, **Ch**, and **ABC**). The propagator $q_i(\mathbf{r},s)$ represents the probability of finding segments s at position $\mathbf{r}$, which satisfies the following modified diffusion equations

$$\frac{\partial q_{AB}(\mathbf{r},s)}{\partial s} = \nabla^2 q_{AB}(\mathbf{r},s) - w_i q_{AB}(\mathbf{r},s), \quad w_i = \begin{cases} w_A, 0 \le s < f_A \\ w_B, f_A \le s \le f_{AB} \end{cases} \tag{5}$$

$$\frac{\partial q_{Ch}(\mathbf{r},s)}{\partial s} = \nabla^2 q_{Ch}(\mathbf{r},s) - w_C q_{Ch}(\mathbf{r},s), \quad 0 \le s \le f_C \tag{6}$$

dx.doi.org/10.1021/jp2021853 |J. Phys. Chem. B 2011, 115, 7550–7560

$$\frac{\partial q_{ABC}(\mathbf{r},s)}{\partial s} = \nabla^2 q_{ABC}(\mathbf{r},s) - w_i q_{ABC}(\mathbf{r},s), \quad w_i = \begin{cases} w_A, 0 \le s < f_A \\ w_B, f_A \le s < f_{AB} \\ w_C, f_{AB} \le s \le 1 \end{cases} \tag{7}$$

subject to the initial condition $q_i(\mathbf{r}, 0)=1$. The backward propagators $q_i^+(\mathbf{r}, s)$ satisfy eqs 5-7, subject to the initial condition $q_i^+(\mathbf{r}_i f_i)=1$ (i=**AB**, **Ch**, and **ABC**).

Minimization of free energy F, with respect to $\phi_i(\mathbf{r})$, $w_i(\mathbf{r})$, and $\xi(\mathbf{r})$, lead to a set of mean-field equations:

$$w_A(\mathbf{r}) = \chi_{AB} N \phi_B(\mathbf{r}) + \chi_{AC} N \phi_C(\mathbf{r}) + \xi(\mathbf{r}) \tag{8}$$

$$w_B(\mathbf{r}) = \chi_{AB} N \phi_A(\mathbf{r}) + \chi_{BC} N \phi_C(\mathbf{r}) + \xi(\mathbf{r}) \tag{9}$$

$$w_C(\mathbf{r}) = \chi_{AC} N \phi_A(\mathbf{r}) + \chi_{BC} N \phi_B(\mathbf{r}) + \xi(\mathbf{r}) \tag{10}$$

where

$$\phi_A(\mathbf{r}) = \frac{V v_{AB}}{Q_{AB}} \int_0^{f_A} ds\, q_{AB}(\mathbf{r},s) q_{AB}^+(\mathbf{r},s) + \frac{V v_{ABC}}{Q_{ABC}} \int_0^{f_A} ds\, q_{ABC}(\mathbf{r},s) q_{ABC}^+(\mathbf{r},s) \tag{11}$$

$$\phi_B(\mathbf{r}) = \frac{V v_{AB}}{Q_{AB}} \int_{f_A}^{f_{AB}} ds\, q_{AB}(\mathbf{r},s) q_{AB}^+(\mathbf{r},s) + \frac{V v_{ABC}}{Q_{ABC}} \int_{f_A}^{f_{AB}} ds\, q_{ABC}(\mathbf{r},s) q_{ABC}^+(\mathbf{r},s) \tag{12}$$

$$\phi_C(\mathbf{r}) = \frac{V v_{Ch}}{Q_{Ch}} \int_0^{f_C} ds\, q_{Ch}(\mathbf{r},s) q_{Ch}^+(\mathbf{r},s) + \frac{V v_{ABC}}{Q_{ABC}} \int_{f_{AB}}^{1} ds\, q_{ABC}(\mathbf{r},s) q_{ABC}^+(\mathbf{r},s) \tag{13}$$

$$\phi_A(\mathbf{r}) + \phi_B(\mathbf{r}) + \phi_C(\mathbf{r}) = 1 \tag{14}$$

The free energy (in units of $k_B T$) can be decomposed into[53−55]

$$F = U - TS = U - T(S_{AB} + S_{Ch} + S_{ABC}) \tag{15}$$

Here, U and S are the internal energy contribution and conformational entropy contribution to free energy, respectively. S_{AB}, S_{Ch}, and S_{ABC} are the conformational entropy of the unbonded **AB** diblock copolymers, unbonded **C** homopolymers, and supramolecular **ABC** terpolymer, respectively. These quantities are given by

$$U = \frac{1}{V} \int d\mathbf{r}\, [\chi_{AB} N \phi_A(\mathbf{r}) \phi_B(\mathbf{r}) + \chi_{AC} N \phi_A(\mathbf{r}) \phi_C(\mathbf{r}) + \chi_{BC} N \phi_B(\mathbf{r}) \phi_C(\mathbf{r})] \tag{16}$$

$$-TS_{AB} = -\frac{v_{AB}}{f_{AB}} \ln \frac{f_{AB} Q_{AB}}{v_{AB} V} - \frac{1}{V} \int d\mathbf{r}\, [w_A(\mathbf{r}) \phi_{A,AB}(\mathbf{r}) + w_B(\mathbf{r}) \phi_{B,AB}(\mathbf{r})] \tag{17}$$

$$-TS_{Ch} = -\frac{v_{Ch}}{f_C} \ln \frac{f_C Q_{Ch}}{v_{Ch} V} - \frac{1}{V} \int d\mathbf{r}\, w_C(\mathbf{r}) \phi_{Ch}(\mathbf{r}) \tag{18}$$

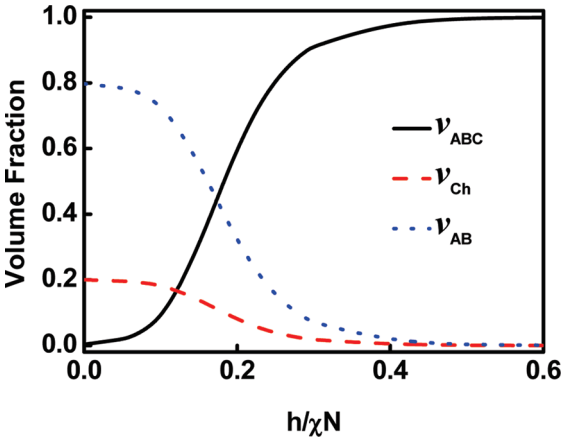

Figure 2. Volume fraction of the three constituent polymers as a function of the bonding strength $h/\chi N$ in **AB** diblock copolymer/**C** homopolymer blends with supramolecular interactions at $v_{C,tot} = 0.2$.

$$-TS_{ABC} = -v_{ABC} \ln \frac{Q_{ABC}}{v_{ABC} V} - \frac{1}{V} \int d\mathbf{r}\, [w_A(\mathbf{r}) \phi_{A,ABC}(\mathbf{r}) + w_B(\mathbf{r}) \phi_{B,ABC}(\mathbf{r}) + w_C(\mathbf{r}) \phi_{C,ABC}(\mathbf{r})] \tag{19}$$

where $\phi_{A,AB}(\mathbf{r})$, $\phi_{B,AB}(\mathbf{r})$, and $\phi_{Ch}(\mathbf{r})$ represent the local densities of **A**, **B**, and **C** blocks in the unbonded polymers at position **r**, whereas $\phi_{A,ABC}(\mathbf{r})$, $\phi_{B,ABC}(\mathbf{r})$, and $\phi_{C,ABC}(\mathbf{r})$ represent the local densities of **A**, **B**, and **C** blocks in supramolecular **ABC** terpolymers at position **r**.

The SCFT equations were solved by using a variant of the algorithm developed by Fredrickson and co-workers.[56−59] Initial field configurations started from a general random state and the diffusion equations (eqs 5-7) were solved via the Baker−Hausdorff operator splitting formula proposed by Rasmussen et al.[60,61] Using the calculated propagators, volume fractions were then evaluated. The chemical potential fields $w_i(\mathbf{r})$ could be updated by using a two-step Anderson mixing scheme.[62] The calculations were carried out in three dimensions. The spatial resolutions were taken as $\Delta x < 0.1 R_g$ and the contour's step size was set to be 0.01. The numerical calculations were carried out until the relative free energy differences in each iteration were smaller than 10^{-6} and the incompressibility condition was achieved. In the calculations the box was optimized for each system to minimize the free energy. The box size corresponding to the lowest free energy upon convergence was chosen as the most appropriate one.[63]

RESULTS AND DISCUSSION

In this work, the self-assembly behavior of diblock copolymer (**AB**)/homopolymer (**C**) blends based on the reversibly supramolecular interactions was examined. The interaction strengths between different blocks were set as $\chi_{AB}N=\chi_{AC}N=\chi_{BC}N=\chi N = 35.0$, which are in the intermediate segregation regime of experimental interests. In a supramolecular **ABC** terpolymer, the volume fraction of **C** blocks f_C was set to be 0.2, and the ratio of **A** block length to **B** block length was set to 1/3, i.e., $f_A = 0.2$ and $f_B = 0.6$. The polymerization degree of supramolecular **ABC** terpolymer is assumed to be $N = 300$. In addition, the $h/\chi N$ was used to describe the supramolecular bonding strength.[47,48]

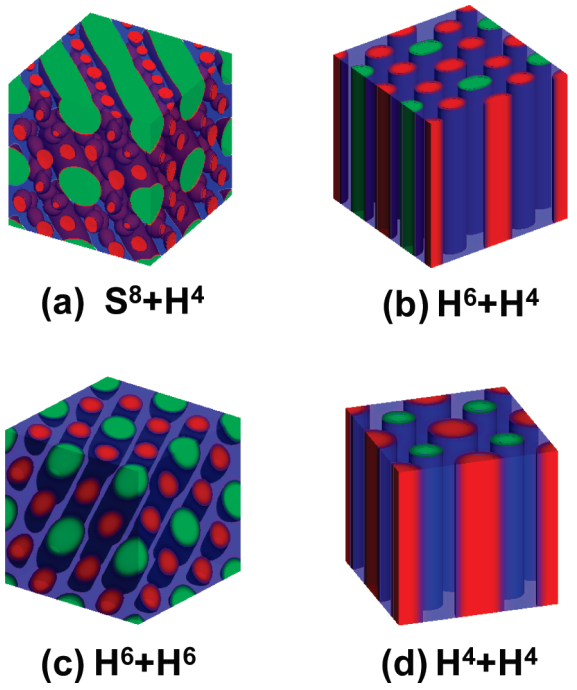

Figure 3. Hierarchical nanostructures self-assembled from the supramolecular **AB** diblock copolymer/**C** homopolymer blends with $v_{C,tot}$ = 0.2 at various bonding strengths: (a) $h/\chi N$ = 0.14, (b) $h/\chi N$ = 0.20, (c) $h/\chi N$ = 0.23, and (d) $h/\chi N$ = 0.30. The red, blue, and green colors represent **A**, **B**, and **C** block-rich domains, respectively.

1. Effects of Bonding Strength on Hierarchical Nanostructure Formation. In this section, the effect of supramolecular bonding strengths $h/\chi N$ on hierarchical nanostructures of **AB**/**C** supramolecular blends was studied. Before the morphological study, we first examined the influence of bonding strength on the volume fraction of the constituent polymers. At equilibrium state, the supramolecular systems consist of three constituent polymers: unbonded **AB** diblock copolymers, unbonded **C** homopolymers, and supramolecular **ABC** terpolymers. The change of bonding strengths can lead to different volume fractions of these three constituent polymers.

Figure 2 shows the volume fractions of three constituent polymers as a function of the bonding strength $h/\chi N$. The total volume fraction of **C** homopolymers $v_{C,tot}$ was set to be 0.20, which is at the stoichiometric ratio (1/1) of **AB** diblock copolymer to **C** homopolymer. When $h/\chi N$ = 0, few reversible supramolecular bond is formed between the diblock copolymers and homopolymers. The supramolecular system is almost a pure mixture of diblock copolymers and homopolymers. When the value of $h/\chi N$ is nonzero, the free end of **B** blocks can be associated with one end of **C** blocks, and therefore the supramolecular **ABC** terpolymers are formed. With increasing the bonding strength, the volume fraction of **ABC** terpolymers increases, while the volume fractions of unbonded **AB** diblock copolymers and **C** homopolymers decrease. Within 0−0.30 range, the volume fraction of **ABC** terpolymers increases rapidly as $h/\chi N$ increases. When the value of $h/\chi N$ is larger than 0.30, the volume fraction of **ABC** copolymers increases slowly, and the **ABC** terpolymers become the major component. As the bonding strength increases beyond 0.40, almost all the **AB** diblock copolymers and **C** homopolymers are connected to form the supramolecular **ABC** terpolymers. As a result, the volume fraction of **ABC** terpolymers

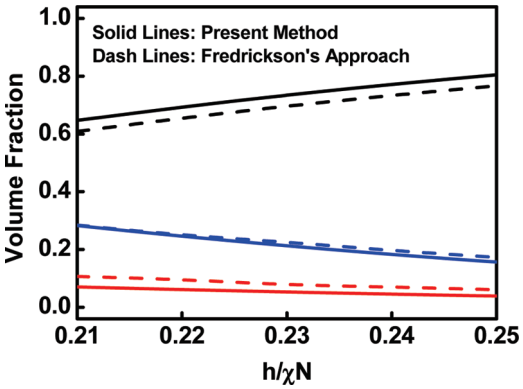

Figure 4. Volume fraction of the three constituent polymers as a function of the bonding strength $h/\chi N$ in **AB** diblock copolymer/**C** homopolymer blends with supramolecular interaction at $v_{C,tot}$ = 0.2. The solid lines are calculated in our simulations, while the dash lines are obtained using Fredrickson's approach. The black, blue, and red lines correspond to the results of the supramolecular **ABC** terpolymer, unbonded **AB** diblock copolymer, and unbonded **C** homopolymer, respectively.

is close to unit, and those of **AB** diblock copolymers and **C** homopolymers are close to zero.

As shown in Figure 2, the variation of the bonding strength leads to a change of the volume fraction of each constituent component. The change of the volume fraction of each component has a pronounced effect on the self-assembly behaviors, and therefore results in a series of nanostructures. Figure 3 shows the representative hierarchically ordered nanostructures at various $h/\chi N$ for the supramolecular **AB**/**C** blends with $v_{C,tot}$ = 0.2. In the figure, the red, blue, and green colors represent the domains rich in **A**, **B**, and **C** blocks, respectively. It was found that the present supramolecular blends prefer to self-assemble into the alternating structures, in which the **A** and **C** blocks form alternating substructures and the **B** blocks occupy the matrix. At weaker bonding strength ($h/\chi N$ = 0.14), the **C** blocks form tetragonally arranged cylinders, while the **A** blocks form octagonally arranged spheres around each **C** cylinder, as shown in Figure 3a. We refer to such structures as $\mathbf{S}^{\mathbf{8}}+\mathbf{H}^{\mathbf{4}}$, where the **S** (sphere) and **H** (cylinder) respectively represent the substructures formed by **A** and **C** blocks. The superscripts **8** and **4** denote the octagonally and tetragonally packing forms of the corresponding substructures, respectively. The designation of other structures also follows this rule. Notably, for the case of $h/\chi N$ = 0.14, the volume fraction of **ABC** terpolymers is relatively lower (see Figure 2). With increasing $h/\chi N$ (0.20), the volume fraction of supramolecular **ABC** terpolymers increases. Under this condition, a $\mathbf{H}^{\mathbf{6}}+\mathbf{H}^{\mathbf{4}}$ structure is formed, where the **C** blocks are organized into tetragonally arranged cylinders surrounded by hexagonally arranged **A** cylinders (Figure 3b). With further increasing $h/\chi N$, the **ABC** terpolymer becomes the major component of the blends. The supramolecular blends self-assemble into the nanostructures of $\mathbf{H}^{\mathbf{6}}+\mathbf{H}^{\mathbf{6}}$ ($h/\chi N$ = 0.23, Figure 3c) and $\mathbf{H}^{\mathbf{4}}+\mathbf{H}^{\mathbf{4}}$ ($h/\chi N$ = 0.30, Figure 3d), respectively, in which the **A** and **C** blocks are organized into alternating hexagonally packed cylinders and alternating tetragonally arranged cylinders. The above nanostructures are shown to be hierarchical. The **C** blocks, both the unbonded and bonded **C** homopolymers, are first separated from **AB** diblocks and form cylinders at large length scales, whereas the **A** blocks of **AB**

dx.doi.org/10.1021/jp2021853 |J. Phys. Chem. B 2011, 115, 7550–7560

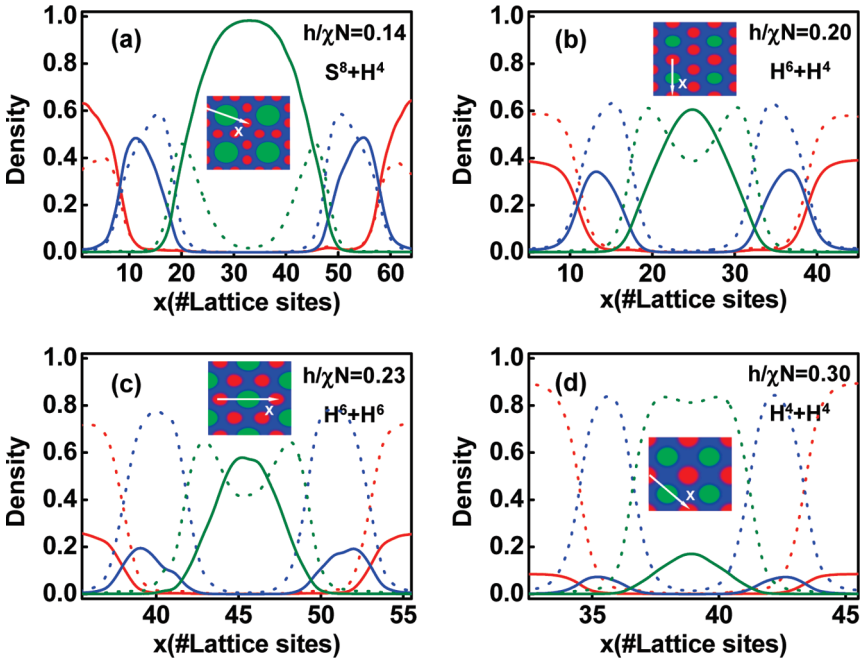

Figure 5. One-dimensional density profiles along the x direction of **A** blocks of unbonded **AB** diblock copolymers $\phi_{A,AB}$ (red solid line) and supramolecular **ABC** terpolymers $\phi_{A,ABC}$ (red dot line), **B** blocks of unbonded **AB** diblock copolymers $\phi_{B,AB}$ (blue solid line) and supramolecular **ABC** terpolymers $\phi_{B,ABC}$ (blue dot line), **C** blocks of unbonded **C** homopolymers ϕ_{Ch} (green solid line) and supramolecular **ABC** terpolymers $\phi_{C,ABC}$ (green dot line) in various nanostructures: (a) S^8+H^4 ($h/\chi N = 0.14$), (b) H^6+H^4 ($h/\chi N = 0.20$), (c) H^6+H^6 ($h/\chi N = 0.23$), and (d) H^4+H^4 ($h/\chi N = 0.30$). The total volume fraction of the **C** components is $\nu_{C,tot} = 0.2$. The insets show the two-dimensional hierarchical nanostructures, where the colors appear as in Figure 3.

diblocks self-assemble into substructures in the **B** matrix at small length scales. From the figures, we can see that as the bonding strength increases, the arrangement of large-length-scale **C** cylinders changes from tetragon to hexagon, and then back to tetragon, while the arrangement of small-length-scale **A** substructures changes from octagon to hexagon to tetragon.

It should be mentioned that, in our simulations we neglected the effect of local fluctuation on the average volume fractions of **ABC**, **AB**, and **C** components, which depends on the bonding strength. The present treatment may give good accuracy for weakly separated structures, however, it could generate some deviations for strongly separated structures. Instead of the present approach, the method proposed by Fredrickson et al. can treat the chemical equilibrium as a function of the space, which is more suitable for studying the nanostructures.[47,48] However, this method may suffer from the difficulty in predicting unknown phase, because the calculations are carried out in grand-canonical ensemble. For this reason, we used the present method instead of Fredrickson's method. To test the validity of the present method, we calculated some representative cases of the present system using Fredrickson's method and compared the results with our predictions. For example, within 0.21−0.25 range of the bonding strength, we found the supramolecular system can self-assemble into alternating hexagonally packed cylinders (H^6+H^6), as shown in Figure 3c. Using this structure as an initial structure, we examined the volume fraction of each component in the framework of Fredrickson. The result is presented in Figure 4. As shown in Figure 4, the relative difference of the volume fractions obtained from these two methods is within 4%, which is relatively small. Therefore, we think that the present method would be appropriate for investigating supramolecular systems, and can capture the essential feature of the self-assembled nanostructures.

To gain the more detailed information about the hierarchical nanostructures, one-dimensional density profile of each block was calculated along the chosen x arrows, which is shown in Figure 5. In the figures, the red, blue, and green lines correspond to the density profiles of **A**, **B**, and **C** blocks, while the solid and dot lines are related to the density profiles from the unbonded and bonded polymers, respectively. From the density profiles, it can be seen that for all the samples the unbonded **C** homopolymers are mainly distributed in the center of **C** domain, and thus push the **C** blocks of the supramolecular **ABC** terpolymers to **B**/**C** interfaces. In addition, due to the restriction of the corresponding molecular chains, the **B** blocks of the supramolecular **ABC** terpolymers are located close to **B**/**C** interface, while the **B** blocks of **AB** diblock copolymers tend to localize at **A**/**B** interface. At weaker bonding strength, as shown in Figure 5a, the **C** domains are mainly occupied by the **C** homopolymers and the **A** domains are mainly formed by the **A** blocks of **AB** diblock copolymers. Therefore, the alternating **A** and **C** substructures are relatively independent, while the supramolecular **ABC** terpolymers bind the **A** and **C** substructures together (S^8+H^4). As the bonding strength increases, the **ABC** terpolymers tend to dominate the formation of **A** and **C** domains, but the **C** homopolymer still swells the **C** domains. As shown in Figure 5b (H^6+H^4) and 5c (H^6+H^6), the **C** domains are greatly swollen by the **C** homopolymers. At stronger bonding strength (H^4+H^4), as shown in Figure 5d, the supramolecular **ABC** terpolymers completely dominate the formation of **A** and **C** substructures, and the **C** homopolymers play a less pronounced effect on the swelling of **C** domains. From above results, we can learn as follows. (a) The **C** homopolymers always swell the **C** domains, and the swollen

dx.doi.org/10.1021/jp2021853 |J. Phys. Chem. B 2011, 115, 7550–7560

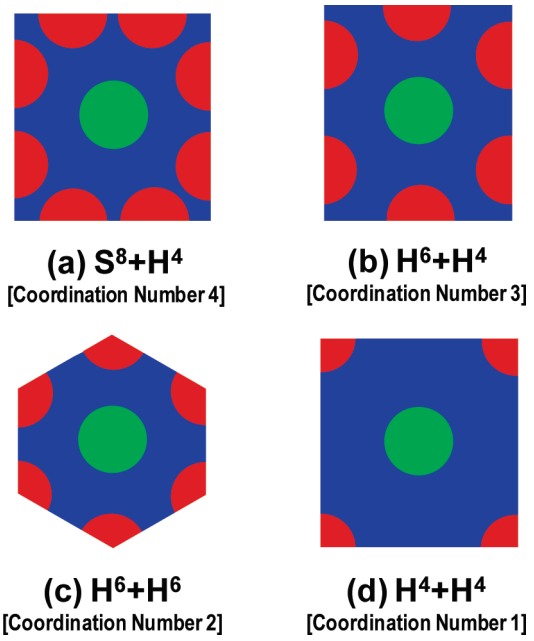

Figure 6. Sketch of the unit cells of (a) the tetragonal **C** cylinders surrounded by octagonal **A** spheres (S^8+H^4), (b) the tetragonal **C** cylinders surrounded by hexagonal **A** cylinders (H^6+H^4), (c) alternating hexagonal cylinders (H^6+H^6), and (d) alternating tetragonal cylinders (H^4+H^4). The color appears as in Figure 3.

effect becomes less marked as the bonding strength increases. (b) At weaker bonding strength, the **A** and **C** substructures are mainly formed by the **AB** diblock copolymers and **C** homopolymers, whereas the supramolecular **ABC** terpolymers behave as adhesives to combine the **A** and **C** substructures together. When the bonding strength is stronger, the formation of **A** and **C** substructures are dominated by the supramolecular **ABC** terpolymers.

From both Figure 3 and Figure 5, we noted that the swelling of **C** domains arisen from the **C** homopolymers has a pronounced effect on the packing forms of **A** cylinders. Figure 6 shows a sketch of the unit cell of the hierarchical structures. The red, blue, and green colors represent the domains rich in **A**, **B**, and **C** blocks, respectively. As shown in Figure 6, the coordination number of **C** cylinders, i.e., the number of **A** substructures around each **C** cylinder, is 4, 3, 2, and 1 for S^8+H^4, H^6+H^4, H^6+H^6, and H^4+H^4, respectively. This means that more coordination **A** cylinders (spheres for S^8+H^4) are required for larger swollen **C** cylinders. The change of coordination numbers in terms of the size of **C** cylinders arises from the interplay of enthalpic and entropic effects. From the viewpoint of enthalpy, the interaction would become more unfavorable as the coordination number decreases, because the **A** and **C** domains are distributed more dispersed with increasing the coordination numbers. Taking $h/\chi N = 0.23$ as an example, we found the H^6+H^6 is stable (Figure 3), where the coordination number is 2. In this sense, the number of surrounding **A** cylinders matches the size of **C** cylinders, and therefore the free energy is optimized. If the microstructures remain H^6+H^4 with larger coordination number, as found at weaker bonding strength ($h/\chi N = 0.20$), the **A** and **B** chains would be stretched in order to accommodate the larger swollen **C** cylinders. In reverse, if the microstructures change to H^4+H^4 with smaller coordination number, as formed at stronger bonding strength ($h/\chi N = 0.30$), the polymeric chains would be relaxed, resulting an increase in configurational entropy. Therefore, at $h/\chi N = 0.23$, the appearance of H^6+H^6 is more entropically favorable than H^6+H^4 and enthalpically favorable than H^4+H^4.

Table 1. Comparison of the Contributions of the Interaction Enthalpy U/nk_BT, Total Configurational Entropy of the Systems $-S/nk_B$, Configurational Entropy of AB Diblock Copolymers $-S_{AB}/nk_B$, Configurational Entropy of C Homopolymers $-S_{Ch}/nk_B$, and Configurational Entropy of ABC Terpolymers $-S_{ABC}/nk_B$ to Total Free Energy F/nk_BT for the Tetragonal C Cylinders Surrounded by Hexagonal A Cylinders (H^6+H^4), the Alternating Hexagonal Cylinders (H^6+H^6), and the Alternating Tetragonal Cylinders (H^4+H^4) at $h/\chi N = 0.23$ and $\nu_{C,tot} = 0.2$

nanostructures	H^6+H^4	H^6+H^6 (stable)	H^4+H^4
coordination number	3	2	1
F/nk_BT	9.314	9.246	9.296
U/nk_BT	3.777	3.804	3.878
$-S/nk_B$	5.537	5.442	5.418
$-S_{AB}/nk_B$	0.850	0.807	0.840
$-S_{Ch}/nk_B$	1.298	1.315	1.288
$-S_{ABC}/nk_B$	3.389	3.320	3.290

To confirm the above assertion, we calculated the free energy of the hierarchical structures including H^6+H^4, H^6+H^6, and H^4+H^4 at $h/\chi N = 0.23$. The free energy was decomposed into the enthalpy U, total configurational entropy $-TS$ of the systems, configurational entropy $-TS_{AB}$ of **AB** diblock copolymer, configurational entropy $-TS_{Ch}$ of **C** homopolymer, and configurational entropy $-TS_{ABC}$ of supramolecular **ABC** terpolymers. The results are given in Table 1. As can be seen from the Table, at $h/\chi N = 0.23$, the H^6+H^6 is stable, but the H^6+H^4 and H^4+H^4 are metastable. With decreasing the coordination numbers, i.e., changing structures from H^6+H^4 to H^6+H^6 to H^4+H^4, the interaction enthalpy increases, while the loss of configurational entropy decreases. The stability of the H^6+H^6 arises from a dramatic increase in configurational entropies of **AB** and **ABC** copolymers as compared to H^6+H^4 and a great decrease in interaction enthalpy as compared to H^4+H^4. These results well prove our arguments aforementioned.

2. Effects of Blend Ratio on Hierarchical Nanostructure Formation. While the above studies were carried out at the stoichiometric ratio of **AB** diblock copolymer to **C** homopolymer, in this section the calculations were turn to investigate the hierarchical nanostructures formed by the system with various blend ratios. We first examined the effect of blend ratio on the volume fraction of three constituent polymers. Figure 7 shows the volume fractions of three constituent polymers as a function of the total volume fraction of **C** component at different bonding strengths. The change of the total **C** volume fraction corresponds to the change of the blend ratio. For all the samples examined, with increasing the total volume fraction of **C** component, the volume fraction of the unbonded **AB** diblock copolymers decreases, while the volume fraction of the supramolecular **ABC** terpolymers first increases to a maximum and then decreases. At stronger bonding strength, as shown in Figure 7a and 7b, the supramolecular **AB**/**C** blend systems can be divided into three regions: region rich in the unbonded **AB** diblock copolymers (region I), region rich in the supramolecular **ABC**

dx.doi.org/10.1021/jp2021853 |*J. Phys. Chem. B* 2011, 115, 7550–7560

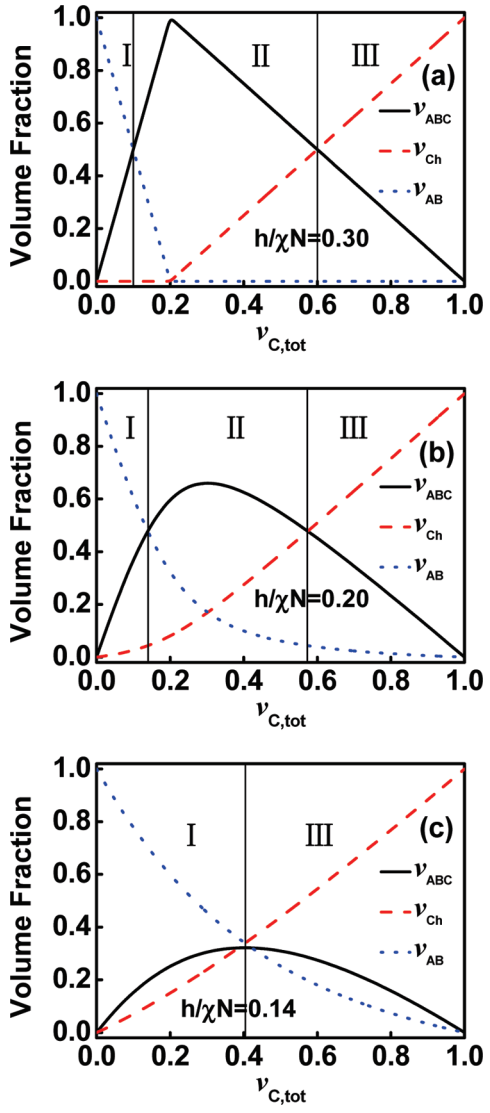

Figure 7. Volume fraction of the three constituent polymers as a function of the total **C** volume fraction for the supramolecular **AB** diblock copolymer/**C** homopolymer blends at various bonding strengths: (a) $h/\chi N = 0.30$, (b) $h/\chi N = 0.20$, and (c) $h/\chi N = 0.14$.

terpolymers (region II), and region rich in the unbonded **C** homopolymers (region III). At weaker bonding strength ($h/\chi N = 0.14$), the three regions become inconspicuous, and only two regions, i.e., region I and region III, were observed, as shown in Figure 7c. This indicates that under this condition, fewer supramolecular **ABC** terpolymers are formed. The maximum volume fraction of the supramolecular **ABC** terpolymers is achieved near stoichiometric ratio, and the corresponding total **C** volume fraction shifts to higher value as the bonding strength decreases.

Figure 8 shows the nanostructures formed by the supramolecular **AB**/**C** blends as a function of total **C** volume fractions. At weaker bonding strength ($h/\chi N = 0.14$), fewer supramolecular **ABC** terpolymers are formed, and the **A** and **C** substructures are dominated by the **A** blocks of **AB** diblock copolymer and **C** homopolymers, respectively (see Figure 7). As shown in Figure 8a, with increasing the total **C** volume fraction, the nanostructures transform from $\mathbf{S}^8+\mathbf{H}^4$ (Figure 8a(1−3)) to **H**+**L** (Figure 8a(4)). These structures exhibit hierarchical features. For example, in the **H**+**L**, the **C** blocks are self-assembled into lamellae at large length scales, while the **A** blocks form small-length-scale cylinders immerged in the lamellar matrix of **B** blocks. At intermediate bonding strength ($h/\chi N = 0.20$), more supramolecular **ABC** terpolymers are formed, which tend to dominate the formation of the hierarchical structures. As shown in Figure 8b(1), the supramolecular **AB**/**C** blends form $\mathbf{H}^6+\mathbf{H}^4$ at lower value of total **C** volume fraction. As $v_{C,tot}$ increases to 0.30, a **S**+**S** nanostructure is produced, where the **C** spheres are tetragonally arranged with several **A** spheres surrounding (Figure 8b(2)). Further increasing $v_{C,tot}$ to 0.4 and 0.5, as shown in Figure 8b(3,4), an alternating lamella ($\mathbf{L}_3$) was observed. At stronger bonding strength ($h/\chi N = 0.30$), the supramolecular **ABC** terpolymers are completely formed in depleted of the **AB** diblock copolymers or **C** homopolymers. The system only comprises two main compositions, depending on the relative amount of **C** homopolymers. At lower total **C** volume fraction (smaller than stoichiometric ratio), the blends consist of the excessive **AB** diblock copolymers and **ABC** terpolymers. In reverse, the blends contain the excessive **C** homopolymers and **ABC** terpolymers. Correspondingly, the $\mathbf{H}^4+\mathbf{H}^4$ nanostructures are formed at $v_{C,tot} = 0.2$, and the $\mathbf{L}_3$ nanostructures are formed at $v_{C,tot} = 0.3$, 0.4, and 0.5, as shown in Figure 8c. Overall, the increase in the total **C** volume fraction leads to the transformation of **C** substructures from cylinders to lamellae.

To look into the structure information on these hierarchical structures in details, we present in Figure 9 the density profile of each block for the samples with various $v_{C,tot}$. As shown in Figure 9, the profiles of the unbonded and bonded **A** blocks are indistinguishable. However, the profiles of the unbonded and bonded **B** blocks show some difference. The bonded **B** blocks prefer to localize at the **B**/**C** interface, while the unbonded **B** blocks tend to distribute at the **A**/**B** interface. The unbonded **C** homopolymers are mainly distributed in the center of **C** domains, and therefore the bonded **C** blocks exhibit a bimodal distribution. The distribution of **C** blocks are greatly dependent on the $v_{c,tot}$. As shown in Figure 9a, in $\mathbf{H}^6+\mathbf{H}^4$ ($v_{C,tot} = 0.2$), the unbonded **C** blocks are weakly segregated with the bonded **C** blocks due to the relatively fewer supramolecular bonds formed. While in the **S**+**S** structures ($v_{C,tot} = 0.3$), as shown in Figure 9b, the bonded **C** blocks show a stronger segregation with the unbonded **C** blocks. However, at $v_{C,tot} = 0.4$ ($\mathbf{L}_3$) (Figure 9c), the separation between the bonded and unbonded **C** homopolymers returns to weaker, as compared to that of **S**+**S** structures. This indicates that a decrease in the interfacial curvature of **C** substructures can relieve the crowding of **C** chains. Therefore, we conclude that an increases in $v_{C,tot}$ can increase the segregation of the unbonded and bonded **C** blocks in **C** domains, and the change of the interfacial curvature of structures can also lead to a change of the separation between the unbonded and bonded **C** blocks.

In the present work, we are mainly concerned about the nanostructures self-assembled from the supramolecular systems. However, for the polymer blends, the existing of macrophase is also an important characteristic of phase behaviors. When the supramolecular interactions are introduced into the blends, the macrophases of supramolecular systems depend on not only the blend ratio, but also the bonding strength. In order to provide an insight into the role of bonding strength in forming macrophase, we used random-phase approximation (RPA) to address the spinodal of macrophase separation. Figure 10 shows a representative result of the spinodals in $h/\chi N$-$v_{C,tot}$ space for

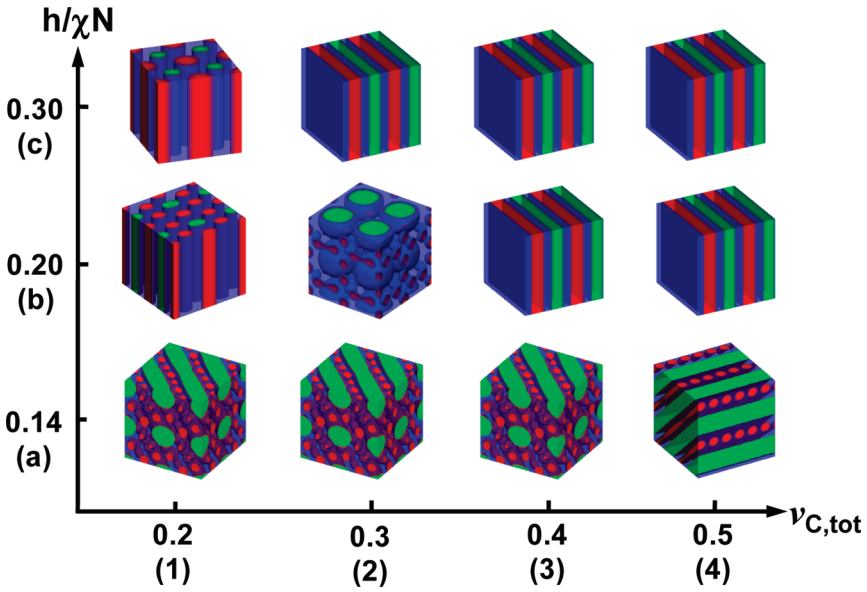

Figure 8. Hierarchical nanostructures as a function of the total **C** volume fraction for the supramolecular **AB** diblock copolymer/**C** homopolymer blends at (a) $h/\chi N = 0.14$, (b) $h/\chi N = 0.20$, and (c) $h/\chi N = 0.30$. The color appears as in Figure 3.

supramolecular blends. As shown in Figure 10, the macrophase separation occurs at higher value of $\nu_{C,tot}$, which means that excessive **C** homopolymers make the macrophase easy to form. As the bonding strength increases, the spinodal of macrophase separation first shifts to higher value of $\nu_{C,tot}$, and then remains unchanged. This suggests that the increase of bonding strength can prevent macrophase separation from occurring, because more supramolecular **ABC** triblock copolymers were formed. When the unbonded **AB** diblock copolymers are depleted at higher bonding strength, the spinodal of macrophase separation is independent of bonding strength since the volume fraction of each component is unchanged. This is the reason why the spinodal of macrophase separation remains unchanged at higher bonding strength. In addition, the spinodal of microphase separation shifts to higher $\nu_{C,tot}$ value and tends to intersect with the spinodal of macrophase separation, as the bonding strength decreases. While the above results are focused on the spinodal of macrophase separation, we rather think the appearance of macrophase between different ordered phases would have similar tendency. The region of macrophase between ordered phases is larger at lower bonding strength and shrinks with increasing bonding strength. When the bonding strength is stronger, the macrophases between ordered phases are less affected by the bonding strength.

3. Comparison with Experimental Observations. In this section, the SCFT results were compared with the experimental results in a qualitative way. So far, there are some reports available in the literatures regarding the **AB** diblock copolymer/**C** homopolymer blends with supramolecular interactions, but these reports are mainly concerned about the polymer misbility.[24−28] Matsushita et al. have investigated the phase behavior of poly(styrene-*b*-2-vinylpyridine) block copolymer (SP)/poly(4-hydroxystyrene) (H) blends.[24,25] Because each P and H can form multiple hydrogen bonds, the P and H chains are well mixed. Therefore, this system cannot separate into hierarchical nanostructures as those in our work, but produce nanostructures as in the diblock copolymer systems. However, in these studies, it was found the excess H can be dissolved into the P/H mixed phase and causes the formation of uniform nanostructures over a wide range of compositions, rather than the macrophase separation. This phenomenon is consistent with our findings. We found that the nanostructures can be formed at higher $\nu_{C,tot}$, for example, the $\mathbf{L_3}$ is formed at $\nu_{C,tot} = 0.5$, where the volume fraction of the excess **C** homopolymers is much higher.

Despite of above report about the phase behaviors of the supramolecular **AB**/**C** blends, people are not so much concerned about the formation of hierarchical nanostructures. While there are no direct study of hierarchical nanostructures from **AB**/**C** blend systems based on supramolecular interactions, there are some studies of hierarchical nanostructures from the self-assembly of the supramolecular **AB**/**CD** blend systems.[20−23] In the **AB**/**CD** blend systems, each **B** and **C** block can form multiple supramolecular interactions. Therefore, the **B** and **C** blocks are mixed very well, and behave as one block in the self-assembly, namely, the supramolecular form of **A**−(**BC**)−**D**. This form has similarity with **A**−**B**−**C** form in our **AB**/**C** blend systems with supramolecular interactions. So it is rational to compare the results of supramolecular **AB**/**C** blends with those of supramolecular **AB**/**CD** blend systems. Fredrickson et al. reported highly ordered square arrays self-assembled from the blends of poly(ethylene oxide)-*b*-poly(styrene-*r*-4-hydroxystyrene) and poly(styrene-*r*-4-vinylpyridine)-*b*-poly(methyl methacrylate), where the poly(styrene-*r*-4-hydroxystyrene) can associate with poly(styrene-*r*-4-vinylpyridine) through hydrogen bonds.[23] In the squared arrays, the poly(ethylene oxide) and poly(methyl methacrylate) blocks form the alternating square arranged cylinders in the matrix formed by poly(styrene-*r*-4-hydroxystyrene) and poly(styrene-*r*-4-vinylpyridine) blocks associated with hydrogen bonds. These square arrays are consistent with our predictions of the $\mathbf{H}^4+\mathbf{H}^4$ in three dimensions, as shown in Figure 3d.

Regarding the supramolecular blends at stoichiometric ratio, almost all the **AB** diblock copolymers and **C** homopolymers are connected to form supramolecular **ABC** terpolymers when the bonding strength is strong, as shown in Figure 2. Therefore, this

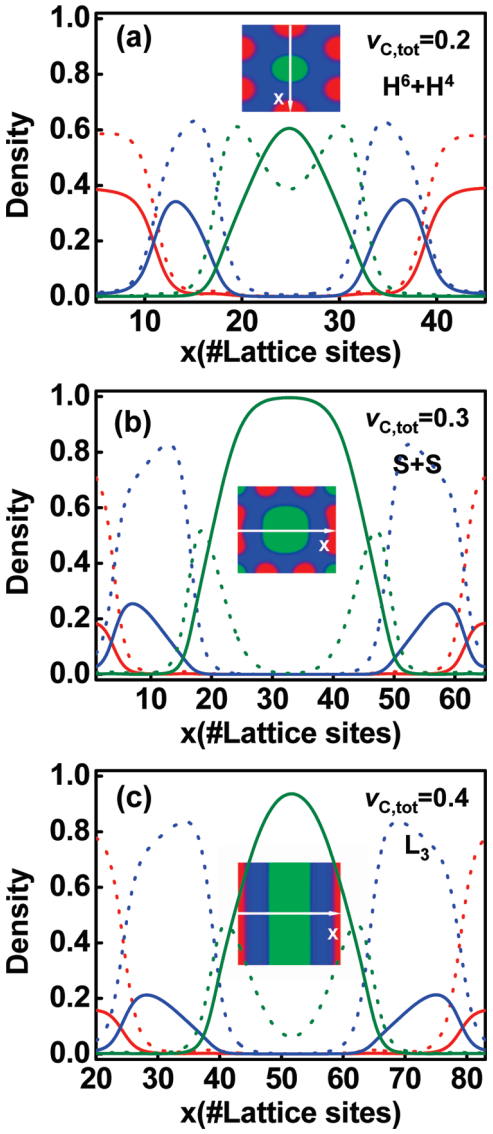

Figure 9. One-dimensional density profiles along x direction of the **A** blocks of the unbonded **AB** diblock copolymers $\phi_{A,AB}$ (red solid line) and supramolecular **ABC** terpolymers $\phi_{A,ABC}$ (red dot line), **B** blocks of the unbonded AB diblock copolymers $\phi_{B,AB}$ (blue solid line) and supramolecular **ABC** terpolymers $\phi_{B,ABC}$ (blue dot line), **C** blocks of the unbonded **C** homopolymers ϕ_{Ch} (green solid line) and supramolecular **ABC** terpolymers $\phi_{C,ABC}$ (green dot line) in various nanostructures of the supramolecular blends with $h/\chi N = 0.20$ at different $v_{C,tot}$: (a) $v_{C,tot} = 0.2$, (b) $v_{C,tot} = 0.3$, and (c) $v_{C,tot} = 0.4$. The inset shows the two-dimensional hierarchical nanostructures, where the color appears as in Figure 3.

system behaves like a melt of **ABC** terpolymers. So far, there are many reports concerning the self-assembly of **ABC** terpolymers. For example, it was reported that the linear **ABC** terpolymers, consisting of end blocks with equal lengths of **A**, **C** and a longer **B** block, are capable of self-assembling into the structures composed of **A** and **C** cylinders tetragonally arranged within **B** matrix.[64−68] This structure is essentially consistent with the H^4+H^4 that observed in the supramolecular blends with higher bonding strength (Figure 3d). However, when the bonding strength is weaker or the blend ratio deviates from the stoichiometric ratio, the system becomes a mixture of supramolecular

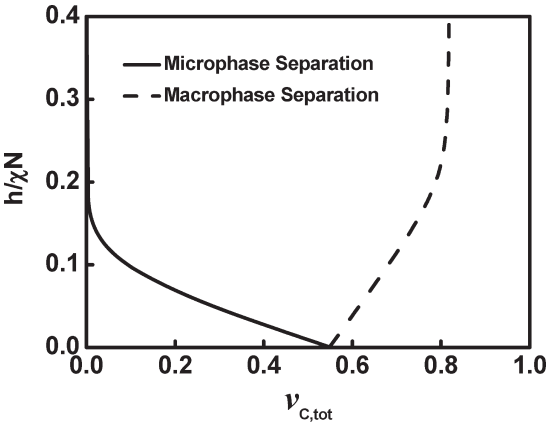

Figure 10. Spinodals in $h/\chi N - v_{C,tot}$ space for **AB** diblock copolymer/**C** homopolymer blends with supramolecular interactions.

ABC terpolymers, unbonded **AB** diblock copolymers, and unbonded **C** homopolymers. As a result, the nanostructures formed by the supramolecular mixtures would be different from those formed by **ABC** copolymers.

In this work, we have investigated the hierarchical nanostructures self-assembled from the supramolecular **AB**/**C** blend systems. It was found that the hierarchical nanostructures are dependent on the bonding strengths and blend ratios. The present calculations can be generalized to other multicomponent blend systems based on supramolecular interactions. The supramolecular multicomponent blend systems have three main advantages, as compared with the conventional diblock copolymer and terpolymer systems. First, these blend systems are capable of self-assembling into hierarchical nanostructures that diblock copolymers cannot achieve. Second, these systems can overcome the difficulty in synthesis of complex copolymers such as terpolymers. Third, these systems are very controllable, where a series of parameters such as blend ratio and bond strength can be easily tuned to produce more rich nanostructures. From the above perspectives, the blend systems based on supramolecular interactions are more suitable for the application in functional materials. The present study can give an insight into the role of supramolecular interaction in generating hierarchically ordered nanostructures, which would be useful in manufacturing high-performance apparatuses such as integrated circuits.

CONCLUSIONS

We employed the real-space self-consistent field theory to explore the hierarchical nanostructures of **AB** diblock copolymer/**C** homopolymer blends based on reversible supramolecular interactions. The reversible bond is formed between the free end of **B** blocks and one end of **C** homopolymers, and therefore the blends consist of the unbonded **AB** diblock copolymers, **C** homopolymers, and supramolecular **ABC** terpolymers. The volume fractions of three constituent polymers depend on the reversible bonding strength and the blend ratio, which play a pronounced influence on the ordered nanostructures. A series of hierarchical structures, such as S^8+H^4, H^6+H^4, H^6+H^6, H^4+H^4, H+L, S+S, and L_3, were observed. With increasing the bonding strength, the volume fraction of the supramolecular **ABC** terpolymers increases, while those of the unbonded **AB** diblock copolymers and **C** homopolymers decrease. As a result, the nanostructures change from S^8+H^4 to H^6+H^4, then to

H^6+H^6, and finally to H^4+H^4 at stoichiometric blend ratio. As the volume fraction of the total **C** component increases, the volume fraction of the supramolecular **ABC** terpolymers first increases to a maximum and then decreases, which lead to a morphological transformation of the self-assembled nanostructures. From the density profiles of these blocks, it was found that the swelling of **C** substructures by the existence of **C** homopolymers results in a variety of arrangements of these substructures in the **B** matrix. The supramolecular blend systems provided a useful method for generating highly complex nanostructures, which would produce periodic nanoporous or related hybrid materials for applications in the fields such as integrated circuit manufacturing.

APPENDIX: RANDOM-PHASE APPROXIMATION

The RPA method, introduced by de Gennes, was deduced for the supramolecular **AB** diblock copolymer/**C** homopolymer blends with supramolecular interactions. The stability limits for the macrophase separation and microphase separation were obtained by calculating $F(\mathbf{q})$,[47,48,69,70] which are given by

$$F(\mathbf{q}) = 1 + 2[\bar{S}_{AB}(\mathbf{q})\chi_{AB} + \bar{S}_{BC}(\mathbf{q})\chi_{BC} + \bar{S}_{AC}(\mathbf{q})\chi_{AC}] + \frac{W_3(\mathbf{q})}{S_3(\mathbf{q})}[2(\chi_{AB}\chi_{BC} + \chi_{BC}\chi_{AC} + \chi_{AC}\chi_{AB}) - (\chi_{AB}{}^2 + \chi_{BC}{}^2 + \chi_{AC}{}^2)] \quad (A1)$$

$$\bar{S}_{ij}(\mathbf{q}) = S_{ij}(\mathbf{q}) - t_i(\mathbf{q})t_j(\mathbf{q})/S_3(\mathbf{q}) \quad (A2)$$

$$t_i(\mathbf{q}) = \sum_{j=1}^{3} S_{ij}(\mathbf{q}) \quad (A3)$$

$$W_3(\mathbf{q}) = S_{AA}(\mathbf{q})S_{BB}(\mathbf{q})S_{CC}(\mathbf{q}) + 2S_{AB}(\mathbf{q})S_{BC}(\mathbf{q})S_{AC}(\mathbf{q}) - [S_{AA}(\mathbf{q})S_{BC}(\mathbf{q})^2 + S_{BB}(\mathbf{q})S_{AC}(\mathbf{q})^2 + S_{CC}(\mathbf{q})S_{AB}(\mathbf{q})^2] \quad (A4)$$

$$S_3(\mathbf{q}) = S_{AA}(\mathbf{q}) + 2S_{AB}(\mathbf{q}) + S_{BB}(\mathbf{q}) + 2S_{BC}(\mathbf{q}) + S_{CC}(\mathbf{q}) + 2S_{AC}(\mathbf{q}) \quad (A5)$$

Here, the correlation functions $S_{ij}(\mathbf{q})$ are

$$S_{AA}(\mathbf{q}) = \nu_{AB}f_{AB}Ng\left(\frac{f_A}{f_{AB}}, x\cdot f_{AB}\right) + \nu_{ABC}Ng(f_A, x) \quad (A6)$$

$$S_{BB}(\mathbf{q}) = \nu_{AB}f_{AB}Ng\left(\frac{f_B}{f_{AB}}, x\cdot f_{AB}\right) + \nu_{ABC}Ng(f_B, x) \quad (A7)$$

$$S_{CC}(\mathbf{q}) = \nu_{Ch}f_CNg(1, x\cdot f_C) + \nu_{ABC}Ng(f_C, x) \quad (A8)$$

$$S_{AB}(\mathbf{q}) = \frac{1}{2}\nu_{AB}f_{AB}N\left[g(1, x\cdot f_{AB}) - g\left(\frac{f_A}{f_{AB}}, x\cdot f_{AB}\right) - g\left(1 - \frac{f_A}{f_{AB}}, x\cdot f_{AB}\right)\right] + \frac{1}{2}\nu_{ABC}N[g(1 - f_C, x) - g(f_A, x) - g(f_B, x)] \quad (A9)$$

$$S_{BC}(\mathbf{q}) = \frac{1}{2}\nu_{ABC}N[g(1 - f_A, x) - g(f_B, x) - g(f_C, x)] \quad (A10)$$

$$S_{AC}(\mathbf{q}) = \frac{1}{2}\nu_{ABC}N[g(1, x) - g(1 - f_C, x) - g(1 - f_A, x) + g(f_B, x)] \quad (A11)$$

$g(f, x)$ satisfies the following equations:

$$g(f, x) = 2[fx + \exp(-fx) - 1]/x^2 \quad (A12)$$

$$x = q^2Na^2/6 = q^2R_g^2 \quad (A13)$$

In the RPA method, the average volume fractions of the supramolecular terpolymers ν_{ABC}, unbonded diblock copolymers ν_{AB}, and homopolymers ν_{Ch} were calculated using eqs 1−3 (in Theoretical Method), which is correlative to the bonding strength $h/\chi N$. For fixed values of N = 300, χN = 35, f_A=f_C = 0.2, and f_B = 0.6, the spinodal in $h/\chi N$-$\nu_{C,tot}$ space was obtained from $F(\mathbf{q}) \rightarrow 0$ at some $\mathbf{q}^*$, where the value of $1/\mathbf{q}^*$ is the measurement of the characteristic length scale of structures. Therefore, when $\mathbf{q}^* = 0$, the spinodal corresponds to macrophase separations since the characteristic length scale of macrophase is infinite. In addition, when $\mathbf{q}^* \neq 0$, the spinodal of microphase transition is obtained because the microphase has a finite characteristic length scale.

AUTHOR INFORMATION

Corresponding Author

*Telephone: +86-21-64253370. Fax: +86-21-64251644. E-mail: jlin@ecust.edu.cn; jplinlab@online.sh.cn.

ACKNOWLEDGMENT

This work was supported by National Natural Science Foundation of China (50925308). Supports from projects of Shanghai municipality (09XD1401400, 0952 nm05100, 08DZ2230500, and B502) are also appreciated.

REFERENCES

(1) Hadjichristidis, N.; Pispas, S.; Floudas, G. A. *Block Copolymers: Synthetic Strategies, Physical Properties, and Applications*; John Wiley & Sons: Hoboken, NJ, 2003.

(2) Jenekhe, S. A. *Polymers for High Technology: Electronics and Photonics*; ACS Symposium Series; Amercian Chemical Society: Washington, DC, 1987; pp 261−269.

(3) Schmidt-Mende, L.; Fechtenkötter, A.; Müllen, K.; Moons, E.; Friend, R. H.; MacKenzie, J. D. *Science* **2001**, *293*, 1119–1122.

(4) Zhou, X.; Kang, S.-W.; Kumar, S.; Kulkarni, R. R.; Cheng, S. Z. D.; Li, Q. *Chem. Mater.* **2008**, *20*, 3551–3553.

(5) Leng, S.; Wex, B.; Chan, L. H.; Graham, M. J.; Jin, S.; Jing, A. J.; Jeong, K.-U.; Van Horn, R. M.; Sun, B.; Zhu, M.; Kaafarani, B. R.; Cheng, S. Z. D. *J. Phys. Chem. B* **2009**, *113*, 5403–5411.

(6) Tyler, C. A.; Qin, J.; Bates, F. S.; Morse, D. C. *Macromolecules* **2007**, *40*, 4654–4668.

(7) Guo, Z.; Zhang, G.; Qiu, F.; Zhang, H.; Yang, Y.; Shi, A.-C. *Phys. Rev. Lett.* **2008**, *101*, 028301.

(8) Yamauchi, K.; Akasaka, S.; Hasegawa, H.; Iatrou, H.; Hadjichristidis, N. *Macromolecules* **2005**, *38*, 8022–8027.

(9) Lee, H.; Chang, T.; Lee, D.; Shim, M. S.; Ji, H.; Nonidez, W. K.; Mays, J. W. *Anal. Chem.* **2001**, *73*, 1726–1732.

(10) Zhu, J.; Jiang, W. *Macromolecules* **2005**, *38*, 9315–9323.

(11) Abetz, V.; Goldacker, T. *Macromol. Rapid Commun.* **2000**, *21*, 16–34.

(12) Vaidya, N. Y.; Han, C. D. *Macromolecules* **2000**, *33*, 3009–3018.

(13) Mao, H.; Arrechea, P. L.; Bailey, T. S.; Johnson, B. J. S.; Hillmyer, M. A. *Faraday Discuss* **2005**, *128*, 149–162.

(14) Hashimoto, T.; Tanaka, H.; Hasegawa, H. *Macromolecules* **1990**, *23*, 4378–4386.
(15) Tanaka, H.; Hasegawa, H.; Hashimoto, T. *Macromolecules* **1991**, *24*, 240–251.
(16) Ibarboure, E.; Bousquet, A.; Toquer, G.; Papon, E.; Rodríguez-Hernández, J. *Langmuir* **2008**, *24*, 6391–6394.
(17) Ye, X.; Sun, Z.; Li, H.; An, L.; Tong, Z. *J. Chem. Phys.* **2008**, *128*, 094903.
(18) Ruokolainen, J.; Mäkinen, R.; Torkkeli, M.; Mäkelä, T.; Serimaa, R.; ten Brinke, G.; Ikkala, O. *Science* **1998**, *280*, 557–560.
(19) Han, Y.; Jiang, W. *J. Phys. Chem. B.* **2011**, *115*, 2167–2172.
(20) Dobrosielska, K.; Takano, A.; Matsushita, Y. *Macromolecules* **2010**, *43*, 1101–1107.
(21) Asari, T.; Matsuo, S.; Takano, A.; Matsushita, Y. *Macromolecules* **2005**, *38*, 8811–8815.
(22) Chen, W.-C.; Kuo, S.-W.; Chang, F.-C. *Polymer* **2010**, *51*, 4176–4184.
(23) Tang, C.; Lennon, E. M.; Fredrickson, G. H.; Kramer, E. J.; Hawker, C J. *Science* **2008**, *322*, 429–432.
(24) Dobrosielska, K.; Wakao, S.; Takano, A.; Matsushita, Y. *Macromolecules* **2008**, *41*, 7695–7698.
(25) Dobrosielska, K.; Wakao, S.; Suzuki, J.; Noda, K.; Takano, A.; Matsushita, Y. *Macromolecules* **2009**, *42*, 7098–7102.
(26) Chen, W.-C.; Kuo, S.-W.; Jeng, U.-S.; Chang, F.-C. *Macromolecules* **2008**, *41*, 1401–1410.
(27) Chen, W.-C.; Kuo, S.-W.; Lu, C.-H.; Jeng, U.-S.; Chang, F.-C. *Macromolecules* **2009**, *42*, 3580–3590.
(28) Chen, S.-C.; Kuo, S.-W.; Jeng, U.-S.; Su, C.-J.; Chang, F.-C. *Macromolecules* **2010**, *43*, 1083–1092.
(29) Coleman, M. M.; Pehlert, G. J.; Painter, P. C. *Macromolecules* **1996**, *29*, 6820–6831.
(30) Tanaka, F.; Ishida, M.; Matsuyama, A. *Macromolecules* **1991**, *24*, 5582–5589.
(31) Tanaka, F.; Ishida, M. *Macromolecules* **1997**, *30*, 1836–1844.
(32) Huh, J.; ten Brinke, G. *J. Chem. Phys.* **1998**, *109*, 789–797.
(33) Huh, J.; Ikkala, O.; ten Brinke, G. *Macromolecules* **1997**, *30*, 1828–1835.
(34) Huh, J.; Jo, W. H. *Macromolecules* **2004**, *37*, 3037–3048.
(35) Angerman, H. J.; ten Brinke, G. *Macromolecules* **1999**, *32*, 6813–6820.
(36) Matsen, M. W.; Thompsom, R. B. *J. Chem. Phys.* **1999**, *111*, 7139–7146.
(37) Matsen, M. W.; Schick, M. *Phys. Rev. Lett.* **1994**, *72*, 2660–2663.
(38) Thompson, R. B.; Ginzburg, V. V.; Matsen, M. W.; Balaze, A. C. *Macromolecules* **2002**, *35*, 1060–1071.
(39) Wang, R.; Li, W.; Luo, Y.; Li, B.; Shi, A.-C.; Zhu, S. *Macromolecules* **2009**, *42*, 2275–2285.
(40) Xu, Y.; Li, W.; Qiu, F.; Yang, Y.; Shi, A.-C. J. *J. Phys. Chem. B* **2010**, *114*, 14875–14883.
(41) Chen, P.; Liang, H.; Shi, A.-C. *Macromolecules* **2008**, *41*, 8938–8943.
(42) Yang, G.; Tang, P.; Yang, Y.; Wang, Q. *J. Phys. Chem. B* **2010**, *114*, 14897–14906.
(43) Ye, X.; Shi, T.; Lu, Z.; Zhang, C.; Sun, Z.; An, L. *Macromolecules* **2005**, *38*, 8853–8857.
(44) Ye, X.; Yu, X.; Shi, T.; Sun, Z.; An, L.; Tong, Z. *J. Phys. Chem. B* **2006**, *110*, 23578–23582.
(45) Zhang, L.; Lin, J. *Macromolecules* **2009**, *42*, 1410–1414.
(46) Wang, L.; Lin, J.; Zhang, L. *Langmuir* **2008**, *25*, 4735–4742.
(47) Feng, E. H.; Lee, W. B.; Fredrickson, G. H. *Macromolecules* **2007**, *40*, 693–702.
(48) Lee, W. B.; Elliott, R.; Katsov, K.; Fredrickson, G. H. *Macromolecules* **2007**, *40*, 8445–8454.
(49) Brunsveld, L.; Folmer, B. J. B.; Meijer, E. W.; Sijbesma, R. P. *Chem. Rev.* **2001**, *101*, 4071–4098.
(50) Ikkala, O.; ten Brinke, G. *Science* **2002**, *295*, 2407–2409.
(51) Matsushita, Y. *Macromolecules* **2007**, *40*, 771–776.
(52) Hoogenboom, R.; Fournier, D.; Schubert, U. S. *Chem. Commun.* **2008**, 155–162.
(53) Wang, L.; Lin, J.; Zhang, L. *Macromolecules* **2010**, *43*, 1602–1609.
(54) Zhu, X.; Wang, L.; Lin, J.; Zhang, L. *ACS Nano* **2010**, *4*, 4979–4988.
(55) Matsen, M. W.; Bates, F. S. *J. Chem. Phys.* **1997**, *106*, 2436–2448.
(56) Fredrickson, G. H. *The Equilibrium Theory of Inhomogeneous Polymers*; Oxford University Press: Oxford, U.K., 2006.
(57) Drolet, F.; Fredrickson, G. H. *Phys. Rev. Lett.* **1999**, *83*, 4317–4320.
(58) Drolet, F.; Fredrickson, G. H. *Macromolecules* **2001**, *34*, 5317–5324.
(59) Ganesan, V.; Fredrickson, G. H. *Europhys. Lett.* **2001**, *55*, 814–820.
(60) Tzeremes, G.; Rasmussen, K. Ø.; Lookman, T.; Saxena, A. *Phys. Rev. E* **2002**, *65*, 041806.
(61) Rasmussen, K. Ø.; Kalosakas, G. *J. Polym. Sci., Part B: Polym. Phys.* **2002**, *40*, 1777–1783.
(62) Eyert, V. *J. Comput. Phys.* **1996**, *124*, 271–285.
(63) Bohbot-Raviv, Y.; Wang, Z.-G. *Phys. Rev. Lett.* **2000**, *85*, 3428–3431.
(64) Mogi, Y.; Kotsuji, H.; Kaneko, Y.; Mori, K.; Matsushita, Y.; Noda, I. *Macromolecules* **1992**, *25*, 5408–5411.
(65) Mogi, Y.; Nomura, M.; Kotsuji, H.; Ohnishi, K.; Matsushita, Y.; Noda, I. *Macromolecules* **1994**, *27*, 6755–6760.
(66) Nakazawa, H.; Ohta, T. *Macromolecules* **1993**, *26*, 5503–5511.
(67) Jung, K.; Abetz, V.; Stadler, R. *Macromolecules* **1996**, *29*, 1076–1078.
(68) Sun, M.; Wang, P.; Qiu, F.; Tang, P.; Zhang, H.; Yang, Y. *Phys. Rev. E* **2008**, *77*, 016701.
(69) Kim, J. K.; Kimishima, K.; Hashimoto, T. *Macromolecules* **1993**, *26*, 125–136.
(70) Ijichi, Y.; Hashimoto, T. *Polym. Commun.* **1988**, *29*, 135–138.